Theor Chim Acta (1996) 93: 269–279

Theoretica Chimica Acta

Electronic structures of superconductors $YBa_2Cu_{3-x}M_xO_y$ (M = Sn, Ni)

Li Ming, Deng Chuanyue, Fu Wentao

Department of Chemistry, Southwest China Normal University, Chongqing 630715, People's Republic of China

Received December 14, 1994/Accepted May 30, 1995

Abstract. Based on the EHMO approach, the energy band structures for superconductors $YBa_2Cu_{3-x}Sn_xO_y$ ($y > 7$) and $YBa_2Cu_{3-x}Ni_xO_y$ ($y < 7$) were calculated in the present paper. The influence of the cation doping at the Cu site in the unit cell and the oxygen content on their electronic structures was studied. The results showed that the cation doping at the Cu site resulted in the great decreases in the bandwidths of the broad anisotropic Cu–O bands and the densities of states. In $YBa_2Cu_{3-x}Sn_xO_y$, however, these decreases are compensated by the increase in the oxygen content caused by the Sn-doping, which results in a small change in the total densities of states. For $YBa_2Cu_{3-x}Ni_xO_y$, the effect of the doping on its electronic structures is dominant. The Ni-doping, therefore, results in a great change in the electronic structures. In addition, the study on the projected densities of states of the Ni-doped system revealed that the 2D Cu–O planes in the Y–Ba–Cu–O system played a dominant role in superconductivity.

Key words: Superconductors – Cation-doping – Oxygen content – $YBa_2Cu_{3-x}M_xO_y$ (M = Sn, Ni)

1 Introduction

In past years, many scientists concentrated their attention, experimentally and theoretically, upon investigations of the influence of the doping and the oxygen content on superconductivity [1–8]. Up to now, many calculations on electronic structures of doping and oxygen vacancy systems have been carried out [9–15]. For the Y–Ba–Cu–O superconductors, it has been known that the doping of many metals, for example, Zn, Ni, Al, and Sn, at the cation sites and the change in the oxygen content have a great effect on their electronic structures and superconductivity although the doping and the small change in the oxygen content do not affect the crystal structures. Generally speaking, substitutions of metals at the Cu site suppress the transition temperature T_c rapidly and the influence of the oxygen content on T_c varies with different superconductors. For most superconducting systems, partial or complete substitutions of cations can generally result in the change in the oxygen content in a unit cell. Therefore, the superconductivity for a system must be influenced both by the doping and by the oxygen content. In many doped superconductors, the doping at the Cu site results in a decrease in

T_c although their oxygen contents increase. For instance, for the Al-doped superconductors $YBa_2Cu_{3-x}Al_xO_y$, T_c is suppressed rapidly although the oxygen content is slightly more than 7. However, for the Sn-doped superconductors $YBa_2Cu_{3-x}Sn_xO_y$, the experiment [7] showed that the increase in the oxygen content y was relatively large as the doping fraction x is raised and that the change in T_c was very little. Obviously, the influence of the cation doping and the oxygen content on the Y–Ba–Cu–O superconducting system varies with doped superconductors.

In order to reveal the role of the cation doping and the oxygen content in the electronic structures of the Y–Ba–Cu–O superconducting system, the electronic energy-band structures for $YBa_2Cu_{3-x}M_xO_y$ (M = Sn, Ni) are investigated in the present paper. As for treatments of partial cation doping and oxygen vacancies, the rigid-band-filling model is often suggested, or an interpolation scheme between two end members is employed in computations by many researchers. Since these treatments are relatively crude and cannot directly reflect the relationship between band structures and the doping fraction x and the oxygen content y, an approximate band-structure treatment based on the EHMO approach will be employed in the present computations.

2 Calculation

Generally speaking, a partially doped system does not have periodicity and the doping often results in a change in the oxygen content in a unit cell. As a result, an approximate band-structure treatment must be used in calculations. For cation-doped systems with the integral oxygen content, the band-structure treatment based on the EHMO approach [16, 17] was given in our previous work [18, 19]. Therefore, it is concisely described only as follows.

In general, three axes a, b, and c of the unit cells of the Cu–O superconductors are large and both the doping atom M^2 and the doped atom M^1 are metals. Therefore, interactions between the doping atom M^2 in a unit cell and the atoms M^1 which are in other unit cells and at the substituted site are small. Thus, it is assumed that (i) these interactions are zero numerically; (ii) the doping process is regarded as the gradual substitution of the doping atom M^2 for the atom M^1 at the fractional ratio x; and (iii) after the doping process was completed, the atom M^1 has been changed into the atom "$(M^1_{1-x}M^2_x)$". Obviously, based on these assumptions, the integrals H_{ij} and S_{ij} in the EHMO approach are all functions of the doping fraction x, that is

$$H_{ij} = H_{ij}(x), \qquad S_{ij} = S_{ij}(x). \tag{1}$$

Let H^1_{ii}, S^1_{ij} and H^2_{ii}, S^2_{ij} be the Coulomb integrals and the overlap integrals before the doping and after the complete substitution, respectively. It is apparent that $H_{ii}(x)$ and $S_{ij}(x)$ obey the boundary conditions

$$H_{ii}(0) = H^1_{ii}, \quad S_{ij}(0) = S^1_{ij}, \quad H_{ii}(1) = H^2_{ii}, \quad S_{ij}(1) = S^2_{ij}. \tag{2}$$

If the numbers of the valence state orbitals for the M^1 and M^2 atoms are equal, $H_{ii}(x)$ and $S_{ij}(x)$ can be approximately expressed as the following forms since Eqs. (2) must be obeyed:

$$\begin{aligned} H_{ii}(x) &= (1-x)H^1_{ii} + xH^2_{ii} + k_1x(1-x)(H^2_{ii} - H^1_{ii}), \\ S_{ij}(x) &= (1-x)S^1_{ij} + xS^2_{ij} + k_2x(1-x)(S^2_{ij} - S^1_{ij}), \end{aligned} \tag{3}$$

where k_1 and k_2 are adjustable parameters and obey the following inequalities

$$-1 \leqslant k_1 \leqslant 1, \qquad -1 \leqslant k_2 \leqslant 1. \tag{4}$$

If the number of the valence state orbitals for the atom M^1, $N1$, and that for the atom M^2, $N2$, are unequal, for instance, $N1 - N2 = N > 0$, let the Coulomb integrals of N orbitals, $H_{\mu\mu}(x)$, be equal to $H^1_{\mu\mu}$ and $S^2_{\mu i} = \delta_{\mu i}$, i.e.,

$$H_{\mu\mu}(x) = H^1_{\mu\mu}(x), \quad S_{\mu i}(x) = (1-x)S^1_{\mu i} + x\delta_{\mu i} + k_2 x(1-x)(\delta_{\mu i} - S^1_{\mu i}),$$
$$(\mu = 1, 2, \ldots, N). \tag{5}$$

It must be emphasized that in this case, good band-structure results could not be obtained if Eqs. (5) were only used when band-structure calculations are carried out. As a consequence, in order to obtain good band structures and densities of states, the total number of electrons in the bands must be raised. The treatment has been given in Ref. [18], which is not described here.

If the oxygen content y is a non-integer, the treatment employed in many studies is usually the rigid-band-filling model or the interpolation between two end members with the integral oxygen content [20]. Since these treatments are very crude and cannot directly reflect the relationship between band-structure results and the oxygen content, an approximate treatment which can be used to calculate the band structures of a system with the non-integral oxygen content must be established.

Let $y = c + z$ in which c is an integer and $0 \leqslant z \leqslant 1$. Obviously, z reflects oxygen vacancies in a unit cell and can be regarded as the number of oxygen atoms that are contained, on the average, by the unit cell except for c oxygen atoms. It is assumed that each of oxygen atoms gets into the given site in the unit cell by degrees. Then, this process can be regarded as the gradual substitution or doping of one oxygen atom for an oxygen vacancy. Based on this assumption, z is the oxygen-doping fraction. Let the Coulomb integrals of the valence orbitals for the doping oxygen atom be $H^0_{\mu\mu}$, their overlap integrals be $S^0_{\mu i}$, and those of oxygen vacancies be equal to zero. Like Eqs. (5), we can obtain

$$H_{\mu\mu}(z) = H^0_{\mu\mu}, \quad S_{\mu i}(z) = \begin{cases} zS^0_{\mu i} + k_p z(1-z)S^0_{\mu i} & (\mu \neq i) \\ 1 & (\mu = i) \end{cases} \quad (\mu \in \text{oxygen}), \tag{6}$$

where k_p is an adjustable parameter and $-1 \leqslant k_p \leqslant 1$. However, in band-structure computations, the number of oxygen atoms cannot be taken as a noninteger but only as an integer $c + 1$. In this case, since $0 \leqslant z \leqslant 1$ the number of oxygen atoms in the unit cell increases, indeed, by $(1 - z)$. This will result in an increase in the total number of electronic energy bands. These bands arising from $(1 - z)$ oxygen atoms may be occupied by electrons, which results in a decrease in the total number of electrons of the unit cell. To obtain satisfactory band-structure results, therefore, the total number of electrons of the unit cell must be increased in computations. In order to increase electrons, an iterative procedure similar to that given in Ref. [18], which is not described here, is employed in the present computations.

It must be pointed out that like the treatment of the cation doping, the above scheme is approximate. It reflects, to be that as it may, directly the relationship between band-structure results and the oxygen content and can provide more details of band structures than can the simple interpolation between two end members (for example, $YBa_2Cu_3O_6$ and $YBa_2Cu_3O_7$) and the rigid-band-filling model.

By use of the above treatment, calculations on the electronic energy-band structures of superconductors $YBa_2Cu_{3-x}M_xO_y$ (M = Sn, Ni) are carried out. In the present computations, two computing schemes are used: (i) M substitutes for Cu(1) in the 1D Cu–O ribbons [M is expressed by M(R)], and (ii) M substitutes for Cu(2) in the 2D Cu–O planes [M is expressed by M(P)]. The structural parameters and the atomic coordinates for $YBa_2Cu_3O_7$ are taken from Ref. [21]. Figure 1 shows the crystal structure of $YBa_2Cu_3O_7$. The change in its structure caused by the doping is neglected because of its small size and minimal structural influence on results obtained by EHMO computations. The atomic orbital ionization potentials and the orbital exponents used in the present calculations are summarized in Table 1. Zhang et al. [7] gave the oxygen contents of the unit cells for $YBa_2Cu_{3-x}Sn_xO_y$ and $YBa_2Cu_{3-x}Ni_xO_y$. For $YBa_2Cu_{3-x}Sn_xO_y$, the oxygen content y increases from 6.9 to 7.34 as the doping fraction x is from 0.0 to 0.3, and for $YBa_2Cu_{3-x}Ni_xO_y$ decreases from 6.9 to 6.80 as x is raised from 0.0 to 0.5. In the present band-structure calculations, oxygen vacancies for $YBa_2Cu_{3-x}Ni_xO_y$ are

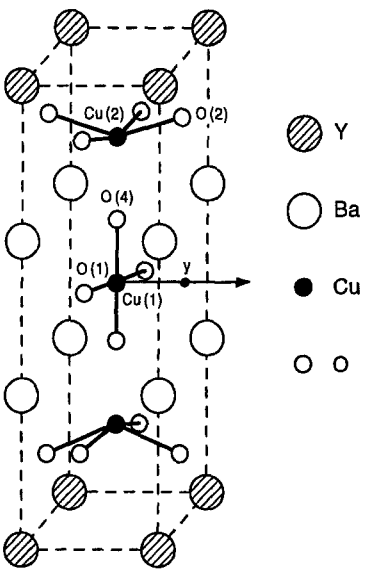

Fig. 1. The crystal structure of $YBa_2Cu_3O_7$

Table 1. EHMO parameters used in the present computations

	$-H_{ii}$ (eV)			Orbital exp.		
	s	*p*	*d*	*s*	*p*	*d*
Y	6.48	5.07	6.38	1.2512	1.2512	3.9896
Cu	9.101	6.06	16.45	1.541	1.541	3.813
Ni	8.893	5.15	15.60	1.471	1.471	3.627
Sn	16.16	8.32		2.12	1.82	
Ba	5.21	3.69		1.25	1.25	
O	32.44	15.86		2.189	2.029	

located at the O(1) site in the unit cell and it is assumed that the eighth oxygen atom for $YBa_2Cu_{3-x}Sn_xO_y$ gets into the y site in the unit cell. Some of the results obtained are listed in Tables 2 and 3, respectively.

3 Results and discussion

Figure 2 shows the band structures of $YBa_2Cu_3O_7$ and $YBa_2Cu_3O_{6.9}$ obtained by employing the treatment given in Sect. 2. It can be seen that as the fraction of the oxygen atom, z, at the O(1) site decreases from 1 to 0.9, the bandwidth of the broad anisotropic band arising from the 1D Cu–O ribbons and crossing the Fermi level E_f becomes small and its band top is gradually displaced towards E_f. Apparently, when $z = 0$, this band is translated into a nonbonding band. In this case, indeed, all the bands related to the O(1) atom are nonbonding bands. If these bands are removed from the band structure, or if the number of electrons occupying these nonbonding bands is added to the unit cell, the band structure is that of $YBa_2Cu_3O_6$. It is clear that the present band-structure treatment does directly relate band-structure results with the oxygen content.

3.1 Band structures

The band structures of $YBa_2Cu_{3-x}Sn_xO_y$ ($y > 7$) and $YBa_2Cu_{3-x}Ni_xO_y$ ($y < 7$) are, respectively, shown in Figs. 3 and 4, in which the Fermi level E_f is placed at the zero of energy.

By comparison to the band structure of $YBa_2Cu_3O_{6.9}$ shown in Fig. 2, it can be seen from Fig. 3 that when the doping fraction x increases from 0.0 to 0.1 the Sn-doping at the Cu(2) site in the 2D Cu–O planes results in the rise of the top of the broad anisotropic band arising from the 1D Cu–O ribbons and in the descent of one of the broad anisotropic band arising from the doped Cu–O planes. The rise of the band top, which increases the bandwidth, is the result of the increase in the oxygen content ($y = 7.28$ at $x = 0.1$), and its descent is caused by the Sn-doping. For the Sn-doping at the Cu(1) site in the 1D Cu–O ribbons, the band structure of $YBa_2Cu_{3-x}Sn_xO_y$ at $x = 0.1$ is almost the same as that of $YBa_2Cu_3O_{6.9}$ near E_f. Of course, it must be emphasized that this result is caused not by the change in the oxygen content but mainly by the Sn-doping at the Cu site. When x varies from 0.1 to 0.3, regardless of whether Sn substitutes partially for the Cu(1) atom or for the

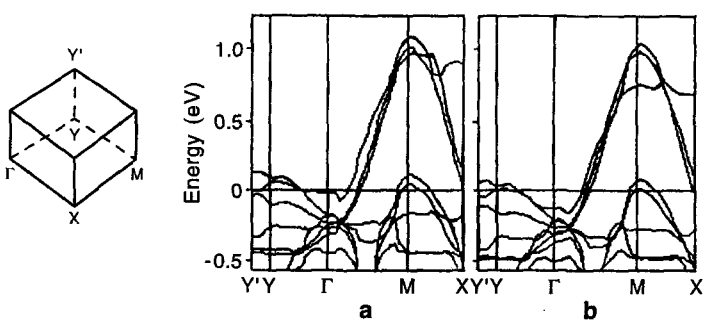

Fig. 2a, b. Band structures for $YBa_2Cu_3O_y$: (a) $YBa_2Cu_3O_7$; (b) $YBa_2Cu_3O_{6.9}$

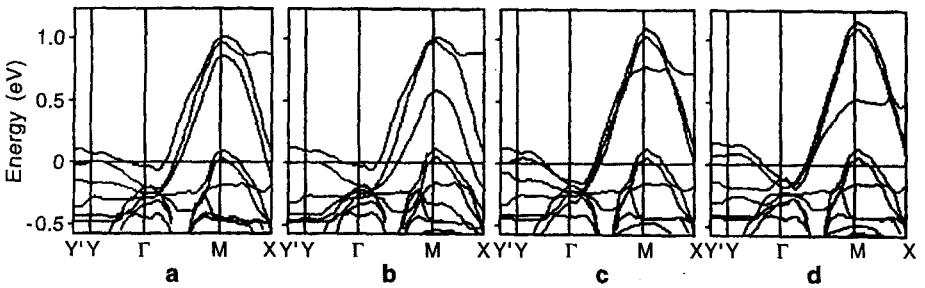

Fig. 3a–d. Band structures for $YBa_2Cu_{3-x}Sn_xO_y$: (a) $YBa_2Cu_{2.9}Sn(P)_{0.1}O_{7.28}$; (b) $YBa_2Cu_{2.7}Sn(P)_{0.3}O_{7.34}$; (c) $YBa_2Cu_{2.9}Sn(R)_{0.1}O_{7.28}$; (d) $YBa_2Cu_{2.7}Sn(R)_{0.3}O_{7.34}$

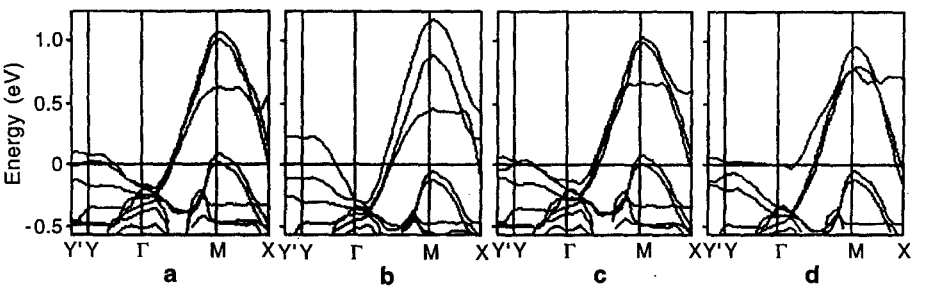

Fig. 4a–d. Band structures for $YBa_2Cu_{3-x}Ni_xO_y$: (a) $YBa_2Cu_{2.9}Ni(P)_{0.1}O_{6.82}$; (b) $YBa_2Cu_{2.5}Ni(P)_{0.5}O_{6.8}$; (c) $YBa_2Cu_{2.9}Ni(R)_{0.1}O_{6.82}$; (d) $YBa_2Cu_{2.5}Ni(R)_{0.5}O_{6.8}$

Cu(2) atom, the top of one broad anisotropic Cu–O band arising either from the Cu–O ribbons or from the Cu–O planes descends continuously towards E_f, which is mostly caused by the Sn-doping. This result is seemingly of no advantage to superconductivity. However, it can be seen from Figs. 2 and 3 that since the oxygen content increases as x is raised ($y = 7.34$ at $x = 0.3$) the band structures near the Fermi surface for the Sn-doping both at the Cu(1) site and at the Cu(2) site are complicated, compared with that of $YBa_2Cu_3O_{6.9}$. This can result in an increase in total densities of states which will be discussed in the next section. The increase in the densities of states is of advantage to superconductivity. As a consequence, as a whole, under the influence of the Sn-doping and the increase in the oxygen content, the change in the transition temperature T_c for the Sn-doped Y–Ba–Cu–O system is very little if the doping fraction x is small. In fact, the experiment [7] shows that $T_c = 90.0$ for $x = 0.1$ and $T_c = 89.0$ for $x = 0.3$. It must be, of course, pointed out that if the oxygen content y in the unit cell of the Sn-doped system retained unchanged as x is raised, T_c would be suppressed rapidly by the doping since its band structures are changed greatly.

For $YBa_2Cu_{3-x}Ni_xO_y$, unlike the Sn-doped system, the oxygen content y decreases from 6.9 to 6.8 as the Ni-doping fraction x increases from 0.0 to 0.5. Since the change in y is small (compared to the oxygen content of $YBa_2Cu_3O_{6.9}$), it is anticipated that the influence of the oxygen content on the electronic structures of $YBa_2Cu_{3-x}Ni_xO_y$ is relatively small (see the next section). As a consequence, the change in its band structures is mainly by the Ni-doping. By comparing Fig. 4 with Fig. 2, it is seen that regardless of whether Ni substitutes partially for Cu(1) or for

Cu(2), the top of one broad anisotropic Cu–O band descends rapidly towards E_f as x is raised. At $x = 0.5$, the bandwidth of this band decreases by about 0.3 eV (about 30% of that of $YBa_2Cu_3O_{6.9}$). In addition, it is also seen that the degree of complication of the band structures near the Fermi surface after the partial doping, unlike the results for $YBa_2Cu_{3-x}Sn_xO_y$, is decreased. This result is mostly caused by the decrease in the oxygen content in the unit cell. It can be, therefore, concluded that the Ni-doping has a great effect on the electronic structures of the Y–Ba–Cu–O superconducting system and its superconductivity, whereas the decrease in the oxygen content also plays some role. In fact, its transition temperature T_c is suppressed rapidly by the Ni-doping, for example, $T_c = 80.0$ for $x = 0.1$ and $T_c = 63.0$ for $x = 0.5$ [7].

3.2 Densities of states

Some results of the densities of states for $YBa_2Cu_{3-x}Sn_xO_y$ and $YBa_2Cu_{3-x}Ni_xO_y$ are summarized in Table 2, in which $N(E_f)$ expresses the total electronic densities of states at the Fermi level E_f, $N_d(E_f)^P_{Cu-O}$ the sums of the projected densities of states at E_f for Cu(2), O(2), and O(3) in the doped Cu–O planes, $N_u(E_f)^P_{Cu-O}$ those for Cu(2), O(2), and O(3) in the undoped Cu–O planes, and $N(E_f)^R_{Cu-O}$ those for Cu(1) and O(1) in the Cu–O ribbons. For the purposes of comparison, the electronic densities of states at E_f for $YBa_2Cu_3O_7$, $YBa_2Cu_{2.7}Sn_{0.3}O_7$, and $YBa_2Cu_{2.5}Ni_{0.5}O_7$ are listed in Table 3.

3.2.1 Sn-doped system

Figure 5 shows the total electronic densities of states (TDOS) near E_f for $YBa_2Cu_{3-x}Sn_xO_y$ at the Sn-doping fraction $x = 0.0$, 0.1, and 0.3. It is clear from Fig. 5 that for each of $YBa_2Cu_{3-x}Sn_xO_y$ there is a strong peak at E_f which arises from the Cu_{3d}–O_{2p} overlaps, regardless of whether Sn substitutes partially for the Cu(1) atom or for the Cu(2) atom (Obviously, the rigid-band-filling model cannot obtain this consequence). It can be seen from Table 2 that the peak heights of these peaks are almost the same as that for $YBa_2Cu_3O_{6.9}$. As x varies from 0.0 to 0.3, $N(E_f)$ for the Sn-doping in the Cu–O planes is hardly changed, and that for the Sn-doping in the Cu–O ribbons decreases only by about 0.5 states/eV-cell. Table 3 demonstrates that if the oxygen content in the unit cell for the Sn-doped superconductors were not increased as x is raised, their $N(E_f)$ would be greatly decreased. For example, for $YBa_2Cu_{2.7}Sn_{0.3}O_7$, its $N(E_f)$ decreases by about 4.0 states/eV-cell. As a consequence, the little change in $N(E_f)$ for the Sn-doped superconductors is caused by the increase in the oxygen content in the unit cell. The total densities of states of a superconducting system are in close relationship with its transition temperature T_c. From the point of view of the BCS theory, T_c is directly proportional to the factor $\exp(-1/N(E_f)V)$. It can be, therefore, concluded that when the Sn-doping fraction x is less than 0.3, the change in T_c for the Sn-doped Y–Ba–Cu–O system is very small, which is in agreement with the experiment.

Going a step further, we can see from Table 2 that when Sn substitutes partially for Cu(2) in the Cu–O planes the projected densities of states of the 2D Cu–O planes for the doped planes, $N_d(E_f)^P_{Cu-O}$, decrease greatly from 3.06 to 1.05 states/eV-cell as x is raised from 0.0 to 0.3, whereas both those for the undoped

Table 2. Densities of states for superconductors $YBa_2Cu_{3-x}M_xO_y$ (M = Sn, Ni)

M	x	y	$N(E_f)$	$N_d(E_f)^P_{Cu-O}$	$N_u(E_f)^P_{Cu-O}$	$N(E_f)^R_{Cu-O}$
Sn(P)	0.0	6.90	7.66	3.06	3.06	0.83
	0.1	7.28	7.63	1.22	3.50	1.76
	0.2	7.34	7.57	1.12	3.68	1.59
	0.3	7.34	7.50	1.05	3.69	1.49
Sn(R)	0.1	7.28	7.27		2.74	0.95
	0.2	7.34	7.46		2.94	0.94
	0.3	7.34	7.10		2.90	0.72
Ni(P)	0.1	6.82	7.13	2.55	3.03	0.81
	0.3	6.80	6.19	2.23	3.01	0.77
	0.5	6.80	5.25	1.12	2.97	0.63
Ni(R)	0.1	6.82	7.46		3.03	0.95
	0.3	6.80	6.35		2.20	1.26
	0.5	6.80	5.31		1.25	1.72

Note: M(P) and M(R) express the M atom at the Cu–O planes and at the Cu–O ribbons, respectively. $N(E_f)$ expresses the total electronic densities of states at the Fermi level E_f, $N_d(E_f)^P_{Cu-O}$ the sums of the projected densities of states at E_f for Cu(2), O(2), and O(3) in the doped Cu–O planes, $N_u(E_f)^P_{Cu-O}$ those for Cu(2), O(2), and O(3) in the undoped Cu–O planes, and $N(E_f)^R_{Cu-O}$ those for Cu(1) and O(1) in the Cu–O ribbons

Table 3. Densities of states for $YBa_2Cu_{3-x}M_xO_7$ (M = Sn, Ni)

	$N(E_f)$	$N_u(E_f)^P_{Cu-O}$	$N(E_f)^R_{Cu-O}$
$YBa_2Cu_3O_7$	8.82	3.01	1.64
$YBa_2Cu_{2.7}Sn(P)_{0.3}O_7$	5.21	2.04	1.43
$YBa_2Cu_{2.7}Sn(R)_{0.3}O_7$	4.43	1.80	0.50
$YBa_2Cu_{2.5}Ni(P)_{0.5}O_7$	6.65	2.49	1.16
$YBa_2Cu_{2.5}Ni(R)_{0.5}O_7$	6.41	2.72	0.42

Note: Sn(P) and Sn(R) or Ni(P) and Ni(R) express the Sn or Ni atom at the Cu–O planes and at the Cu–O ribbons, respectively. $N(E_f)$ expresses the total electronic densities of states at the Fermi level E_f, $N_u(E_f)^P_{Cu-O}$ the sums of the projected densities of states at E_f for Cu(2), O(2), and O(3) in the undoped Cu–O planes, and $N(E_f)^R_{Cu-O}$ those for Cu(1) and O(1) in the Cu–O ribbons

Cu–O planes, $N_u(E_f)^P_{Cu-O}$, and the projected densities of states for the Cu–O ribbons, $N(E_f)^R_{Cu-O}$ increase from 3.06 to 3.69 for $N_u(E_f)^P_{Cu-O}$ and from 0.83 to about 1.5 for $N(E_f)^R_{Cu-O}$. In addition, the projected densities of states for other atoms in the unit cell are, to some extent, also increase. Apparently, the decrease in $N_d(E_f)^P_{Cu-O}$ is mostly caused by the Sn-doping. However, the increases in $N_u(E_f)^P_{Cu-O}$ and $N(E_f)^R_{Cu-O}$ are caused by the increase in the oxygen content because the calculations show that both $N_u(E_f)^P_{Cu-O}$ and $N(E_f)^R_{Cu-O}$ for $YBa_2Cu_{3-x}Sn(P)_xO_7$ decrease with the increase in the Sn-doping fraction x by comparison with that of $YBa_2Cu_3O_7$. At $x = 0.3$, for instance, $N_u(E_f)^P_{Cu-O}$ decreases by about 1.0 states/eV-cell and $N(E_f)^R_{Cu-O}$ by about 0.2 states/eV-cell (see Table 3). As a result, the decrease in $N_d(E_f)^P_{Cu-O}$ for $YBa_2Cu_{3-x}Sn(P)_xO_y$ is compensated by the increase in the projected densities of states of other atoms in

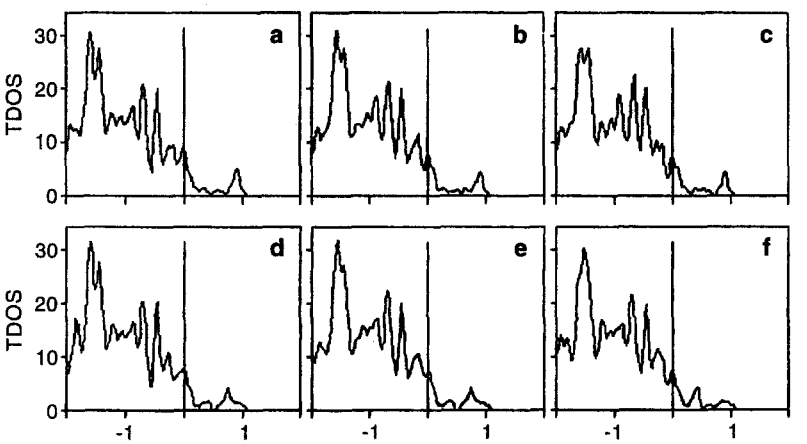

Fig. 5a–f. Total densities of states for $YBa_2Cu_{3-x}Sn_xO_y$: (a) $YBa_2Cu_3O_7$; (b) $YBa_2Cu_{2.9}Sn(P)_{0.1}O_{7.28}$; (c) $YBa_2Cu_{2.7}Sn(P)_{0.3}O_{7.34}$; (d) $YBa_2Cu_3O_{6.9}$; (e) $YBa_2Cu_{2.9}Sn(R)_{0.1}O_{7.28}$; (f) $YBa_2Cu_{2.7}Sn(R)_{0.3}O_{7.34}$

the unit cell, which results in the unchanged total densities of states for $YBa_2Cu_{3-x}Sn(P)_xO_y$. For the Sn-doping in the Cu–O ribbons, it is seen from Table 2 that the changes in $N_u(E_f)^P_{Cu-O}$ and $N(E_f)^R_{Cu-O}$ are very small by comparison with those of $YBa_2Cu_3O_{6.9}$. Like the Sn-doping at the Cu(2) site, this result is also caused by the increase in the oxygen content since both $N_u(E_f)^P_{Cu-O}$ and $N(E_f)^R_{Cu-O}$ of $YBa_2Cu_{3-x}Sn(R)_xO_7$, compared to those of $YBa_2Cu_3O_7$, decrease greatly with the increase in x. Therefore, the total densities of states for $YBa_2Cu_{3-x}Sn(R)_xO_y$ are basically unchanged.

As above, it can be concluded that the oxygen content plays an important role in the electronic structures for the Sn-doped Y–Ba–Cu–O superconductors. The great decrease in the densities of states caused by the doping is compensated by their increase caused by the increase in the oxygen content, which results in the unchanged total densities of states.

3.2.2 Ni-doped system

TDOS for $YBa_2Cu_{3-x}Ni_xO_y$ ($y < 7$) at $x = 0.1$, 0.3, and 0.5 are shown in Fig. 6. In the above discussion on the densities of states of $YBa_2Cu_3O_{6.9}$, it has been indicated that in its total densities of states, there is a strong Cu_{3d}–O_{2p} peak at E_f. For the Ni-doped system, it is seen from Fig. 6 that regardless of whether Ni substitutes partially for Cu(1) or for Cu(2), this Cu_{3d}–O_{2p} peak is displaced downward and departs from E_f gradually as x is raised. This result has a great influence on the total densities of states at E_f, $N(E_f)$. It is shown by Table 2 that with x from 0.0 to 0.5, $N(E_f)$ for $YBa_2Cu_{3-x}Ni(P)_xO_y$ decreases by about 2.4 states/eV-cell and that for $YBa_2Cu_{3-x}Ni(R)_xO_y$ by about 2.8 states/eV-cell. Obviously, the Ni-doping results in a great decrease in $N(E_f)$. Since $N(E_f)$ is in close relationship with the transition temperature, T_c for the Ni-doping Y–Ba–Cu–O system is suppressed rapidly as x is raised. Further, we see from Table 3 that $N(E_f)$ for $YBa_2Cu_{2.5}Ni(P)_{0.5}O_7$ decreases by about 2.2 states/eV-cell and that for $YBa_2Cu_{2.5}Ni(R)_{0.5}O_7$ by about 2.4 states/eV-cell. It is apparent that

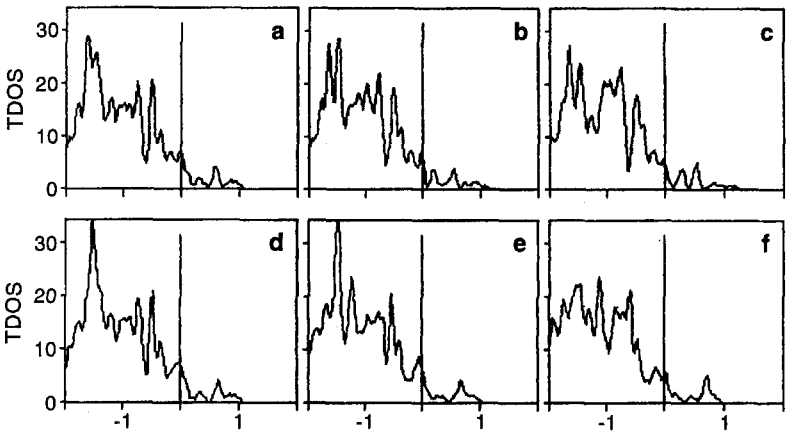

Fig. 6a–f. Total densities of states for $YBa_2Cu_{3-x}Ni_xO_y$: (a) $YBa_2Cu_{2.9}Ni(P)_{0.1}O_{6.82}$; (b) $YBa_2Cu_{2.7}Ni(P)_{0.3}O_{6.8}$; (c) $YBa_2Cu_{2.5}Ni(P)_{0.5}O_{6.8}$; (d) $YBa_2Cu_{2.9}Ni(R)_{0.1}O_{6.82}$; (e) $YBa_2Cu_{2.7}Ni(R)_{0.3}O_{6.8}$; (f) $YBa_2Cu_{2.5}Ni(R)_{0.5}O_{6.8}$

the decrease in $N(E_f)$ for $YBa_2Cu_{3-x}Ni_xO_7$ is almost equal to that for $YBa_2Cu_{3-x}Ni_xO_y$ ($y < 7$). Therefore, the change in the densities of states for the Ni-doped system is mostly caused by the Ni-doping, whereas the decrease in the oxygen content has only a small effect. Furthermore, it can be seen from Table 2 that for the Ni-doping at the Cu(2) site, $N_d(E_f)^P_{Cu-O}$ for the doped Cu–O planes decreases greatly by about 2.0 states/eV-cell with x from 0.0 to 0.5, whereas $N_u(E_f)^P_{Cu-O}$ for the undoped Cu–O planes and $N(E_f)^R_{Cu-O}$ of the Cu–O ribbons almost retain unchanged. In the Ni(R)-doped system, $N_u(E_f)^P_{Cu-O}$ is also changed greatly, decreasing by about 1.8 states/eV-cell. These results demonstrate that the effect of the Ni-doping on the 2D Cu–O planes is much larger than on the 1D Cu–O ribbons. In other words, the densities of states near E_f are more sensitive to the Cu–O planes than to the Cu–O ribbons. As a consequence, the 2D Cu–O planes play a dominant role in the electronic structures of the Y–Ba–Cu–O system and its superconductivity, which is in agreement with the conclusion obtained in our previous work [18, 19].

4 Conclusion

To summarize, the present band-structure treatment based on the EHMO approach has modeled cation doping and oxygen vacancies at any site in a unit cell. It is known from the above discussion that this treatment obtains nonrigid-band behavior. Although relatively approximate, it reflects directly the relationship between band-structure results and the doping fraction and the oxygen content. So far as the degree of approximation of this treatment goes, it gives, indeed, average band structures and average densities of states. But it is totally unsimilar to the simple interpolation between two end members and can provide more details of band structures. It can be, therefore, employed to investigate doped systems with oxygen vacancies.

The studies on the band structures and the densities of states of Sn-doped superconductors $YBa_2Cu_{3-x}Sn_xO_y$ ($y > 7$) reveal that the great chagnes in their

electronic structures caused by the doping are compensated by the increase in the oxygen content caused by the doping. The total electronic densities of states at the Fermi level E_f almost retain unchanged. For Ni-doped superconductors $YBa_2Cu_{3-x}Ni_xO_y$ ($y < 7$), the influence of the doping on the electronic structures is dominant. The Ni-doping results in the great decreases in the bandwidths of the broad anisotropic Cu–O bands and the total densities of states. In addition, the study on the projected densities of states shows that the 2D Cu–O planes in the unit cell play a dominant role in superconductivity.

Acknowledgments. This work was supported by the Science Foundation of Chongqing City, PRC.

References

1. Jorgensen JD, Schuttler HB, Hinks DG (1987) Phys Rev Lett 58:1024
2. Tokura Y, Takadgi H, Uchida S (1989) Nature 337:345
3. Takadgi H, Uchida S, Tokura Y (1989) Phys Rev Lett 62:1197
4. Torrance JB et al. (1989) Phys Rev B40:8872
5. Xiao G, Cieplak MZ, Gavrin A et al. (1988) Phys Rev Lett 60:1446
6. Beyers R, Shaw TM (1989) Solid State Phys 42:135
7. Zhang H, Zhao Y, Zhou XY et al. (1990) Phys Rev B42:2253
8. Zhang H, Zhao Y, Zhou XY et al. (1989) Solid State Commun 71:934
9. Burdett JK, Kulkarni GV, Levin K (1987) Inorg Chem 26:3650
10. Kasowski RV, Hsu WY, Herman F (1987) Solid State Commun 63:1077
11. Kasowski RV, Hsu WY, Herman F (1987) Phys Rev B36:7248
12. Pickett WE, Krakauer H, Papaconstantopoulos DA et al. (1987) Phys Rev B35:7252
13. Schwarz K (1987) Solid State Commun 64:421
14. Papaconstantopoulos DA, Pickett WE et al. (1988) Phys Rev Lett 61:211
15. Pickett WE (1989) Rev Mod Phys 61:433
16. Whangbo MH et al. (1978) J Am Chem Soc 100:6093
17. Whangbo MH et al. (1979) Proc Roy Soc (London) 366A:23
18. Li Ming (1994) Int J Quantum Chem 50:233
19. Li Ming, Wu Xiaoping (1994) Theor Chim Acta 89:169
20. Beno MA, Soderholm L, Capone DW et al. (1987) Appl Phys Lett 51:57
21. Herman F, Kasowaki RV, Hsu WY (1987) Phys Rev B36:6904